Journal of Agricultural Machinery

Homepage: https://jame.um.ac.ir

Research Article
Vol. 15, No. 1, Spring 2025, p. 1-22

Artificial Neural Network (ANN) Modeling of Plasma and Ultrasound-assisted Air Drying of Cumin Seeds

M. Namjoo [1], M. Moradi [2*], M. A. Nematollahi [2], H. Golbakhshi [3]

1- Department of Mechanical Engineering of Biosystems, Faculty of Agriculture, University of Jiroft, Jiroft, Iran
2- Department of Biosystems Engineering, College of Agriculture, Shiraz University, Shiraz, Iran
3- Department of Mechanical Engineering, University of Jiroft, Jiroft, Iran
(*- Corresponding Author Email: moradih@shirazu.ac.ir)

Received: 06 December 2023
Revised: 12 April 2024
Accepted: 11 May 2024
Available Online: 11 February 2025

How to cite this article:
Namjoo, M., Moradi, M., Nematollahi, M. A., & Golbakhshi, H. (2025). Artificial Neural Network (ANN) Modeling of Plasma and Ultrasound-assisted Air Drying of Cumin Seeds. *Journal of Agricultural Machinery, 15*(1), 1-22. https://doi.org/10.22067/jam.2024.85744.1209

Abstract

In this study, the air drying of cumin seeds was boosted by cold plasma pre-treatment (CPt) followed by high-power ultrasound waves (USp). To examine the impact of included effects, different CP exposure times (0, 15, and 30 s), sonication powers (0, 60, 120, and 180 W), and drying air temperatures (30, 35, and 40 ^{o}C) were selected as input variables. A series of well-designed experiments were conducted to evaluate drying time, effective moisture diffusivity, and energy consumption, as well as color change and rupture force of dried seeds for each drying program. Numerical investigations can effectively bypass the challenges associated with experimental analysis. Therefore, the wavelet-based neural network (WNN), the multilayer perceptron neural network (MLPNN), and the radial-basis function neural network (RBFNN), as three well-known artificial neural networks models, were used to map the inputs and output data and the results were compared with the Multiple Quadratic Regression (MQR) analysis. According to the results, the WNN model with an average correlation coefficient of $R^2 > 0.92$ for the train data set, and $R^2 > 0.83$ for the test data set provided the most beneficial tool for evaluating the drying process of cumin seeds.

Keywords: Artificial neural network, Cold plasma, Cumin seeds, Drying, Ultrasound

Nomenclature	
MR	Moisture ratio (-)
M_t	Time-dependent moisture content of the seeds (-)
M_0	Primary moisture content of the seeds (-)
M_e	Equilibrium Moisture content (-)
D_{eff}	Diffusion coefficient (m^2s^{-1})
t	Drying time (min)
M	Moisture concentration (-w.b.)
ΔE	Total color change (-)
L^*	Whiteness/darkness (-)
a^*	Redness/greenness (-)
b^*	Yellowness/blueness (-)
L	Half thickness of the drying body (m)
y	Dependent variable (-)
x	Independent variable (-)
β	Constant term (-)

https://doi.org/10.22067/jam.2024.85744.1209

Introduction

Cumin seed (*Cuminum Cyminum* L.) is a seed from the *Apiaceae* family, formerly called Umbelliferae. Umbelliferous seeds are rich in essential oil content, offering valuable applications in the food, perfume, cosmetic, and pharmaceutical sectors of the industry (Guo, An, Jia, & Xu, 2018; Merah *et al.*, 2020). Thanks to the high levels of petroselinic acid and other bioactive molecules in cumin seed, it is valued for its medicinal and therapeutic properties. Moreover, cumin seeds are widely used as a spice in cooking due to their strong aroma and warm bitterish taste (Namjoo, Moradi, Niakousari, & Karparvarfard, 2022), dominated by the flavor compound cumin aldehyde. The drying process has a crucial role in the production of high-quality cumin seeds. This process also reduces the bulk volume and facilitates the transportation and disposal of end-products (Khalo ahmadi, Roustapour, & Borghaee, 2022). In initial drying, the freshly harvested plants are exposed to sunlight for easier separation of cumin seeds. Then, the drying process should be continued, whether by sun or dryer, until the final level of moisture content of seeds reaches 10% on the wet basis (Namjoo, Dibagar, Golbakhshi, Figiel, & Masztalerz, 2024).

The essential oil of cumin has outstanding chemical and biological characteristics which may be badly affected by heating (Guo *et al.*, 2018). Shortening the drying period is an effective approach to minimize the exposure time of samples to the harmful effects of dehydration. Therefore, to accelerate the drying process and preserve the natural characteristics of the samples, some physical-based treatments, prior to the main single or hybrid drying procedures, have been investigated by researchers (Tabibian, Labbafi, Askari, Rezaeinezhad, & Ghomi, 2020).

The cold plasma (CP) and the ultrasound waves (US) are two physical-field techniques which have widespread applications in the drying process. These non-thermal and non-chemical technologies can improve the performance of drying systems, without leaving any adverse effects on chemical structure and physical properties of samples (Zhou *et al.*, 2020). By exposing the food materials to CP, some surface reactions occur and alters the surface topography of the skin layer (Miraei Ashtiani et al., 2020; Osloob, Moradi, & Niakousari, 2023). The internal microstructure may also be changed by propagation of high-power ultrasound waves during the air-drying process. As a result, when the CP pretreated samples are dried in a US-assisted air drying system, the effective moisture diffusivity significantly increases, resulting in a higher rate of water evaporation compared to the performance of single dryers (Moghimi, Farzaneh, & Bakhshabadi, 2018; Shashikanthalu, Ramireddy, & Radhakrishnan, 2020).

Besides the effective moisture diffusivity and drying time, the amount of consumed energy, as well as the total color change, and rupture force of end-products may also be evaluated for assessing the performance of the upgraded system (Moradi, Ghasemi, & Azimi-Nejadian, 2021; Namjoo, Moradi, Niakousari, *et al.*, 2022). In this case, conducting a comprehensive experimental investigation appears to be daunting and could require significant time and resources. Forecasting the dehydration process of various crops by numerical modeling is a more practical approach for improving the performance of the drying systems (Sun, Zhang, & Mujumdar, 2019).

Based on the results of the limited number of experiments, some regression-based methods such as multiple linear regressions (MQR) can establish a proper relationship between inputs and outputs and predict the performance of a system for non-inspected drying conditions (Meerasri & Sothornvit, 2022). The artificial neural network (ANN) is another category of data-driven methods that is developed based on the biological neural systems in the human body. This class of computing models is also coupled with artificial intelligence to improve the correlation between inputs and outputs. In the

nonlinear problems with more than one input parameter, ANN can readily forecast the values of desired output variables (Kaveh, Abbaspour Gilandeh, Amiri Chayjan, & Mohammadigol, 2019). Recently, ANN has been widely used to investigate the drying process of various crops, including pumpkin seeds (Dhurve, Tarafdar, & Arora, 2021), basil seeds(Amini, Salehi, & Rasouli, 2021), ginkgo biloba seeds (Bai, Xiao, Ma, & Zhou, 2018), potato slice (Rezaei, Behroozi-Khazaei, & Darvishi, 2021), pistachio nuts, squash, and cantaloupe seeds (Mohammad Kaveh, Chayjan, & Khezri, 2018), mushroom slices (Liu *et al.*, 2019), and green tea leaves (Kalathingal, Basak, & Mitra, 2020).

As mentioned earlier, in case of cumin seed drying, the quality of end-products, the energy costs, and production rate may significantly improve by CP pretreatment followed by ultrasound-assisted air drying. To the best knowledge of authors, there is no predicting model developed for estimating the positive influence of cold plasma and high-power ultrasound waves on the drying of cumin seeds. To fill this gap, the drying of cumin seeds is investigated in the current research and through several experiments, drying time, effective moisture diffusivity, energy consumption, total color change, and rupture force (as the output variables) were measured for different drying air temperature, CP exposure time (CPt), and ultrasound power (USp). Then, the wavelet-based neural network (WNN), the multilayer perceptron (MLP), and radial basis function (RBF) neural networks were employed for mapping the input and output data. For evaluating the accuracy of predictions, the results of multiple linear regressions (MQR) were also obtained and compared with the results of neural network-based models.

Materials and Methods

Sample Preparation and CP Pretreatment

In this research, freshly harvested cumin seeds were provided from a local farm in Khatam County in Yazd province, central Iran to certify genetic purity. The samples were characterized by longitudinal ridges, are yellow-brown, and have 69.4% (d.b.) initial moisture content. For uniform distribution of moisture throughout the samples, the healthy seeds were wrapped in polythene plastic bags and kept refrigerated at 4±1 °C and relative humidity of 53±1%. The CP device (Nik Plasma Tech Co., Tehran, Iran) in the excitation mode of Dielectric Barrier Discharge (DBD) was used to pretreat the seeds. Before each drying run, 60 g of cumin seed sample was used for CP pretreatment at different exposure times of 15 or 30 s. After CP pretreatment, 10 g of the sample was separated to determine the moisture content as well as to evaluate the color characteristics of the pretreated seeds to ensure that no significant alteration occurred in the initial moisture level and color quality of the samples. The rest of the pretreated sample, 50 g, was placed in the drying chamber and exposed to different drying programs for further analysis. Runs with no CP pretreatment (CPt: 0 s) were also conducted as control experiments. At the laboratory site, the temperature and relative humidity of the ambient air were 25 °C and 50%, respectively.

Ultrasound-Assisted Air-Drying Process

To conduct the main drying experiment, a hybrid ultrasound-assisted convective dryer was constructed at the Faculty of Agriculture, Shiraz University, Shiraz, Iran, as demonstrated in Figure 1. The drying unit is equipped with a centrifugal fan (2200 RPM, 550 m^3 h^{-1}, and BEF-14-7V2SP), controller unit of input variables, multifunction monitoring system (humidity, temperature, energy, and weight), electrical heater (including 3 kW electrical heating coils), drying chamber, sonication unit (20 kHz), and inverter. The sonication unit (Farasot Zagros Co., Iran) contained a 1200 W generator, power meter (Model Delta power, Ziegler Co., Germany), transducer, and horn. The piezoelectric transducer was made up of four piezoceramic rings with an outer diameter of 50 mm, an inner diameter of 20 mm, and a thickness of 6 mm. Additionally, a thermal

velocity probe was used to measure the linear air flow rate. The forward one-phase centrifugal fan propelled the drying air toward the electric heater, warming it to achieve the desired temperature. For online moisture content control, the samples enclosed in the cylindrical mesh basket were weighed every 3 minutes. A detailed description of the main hybrid drying unit can be found in Namjoo *et al.*, (2022). Each drying trial lasted until the final moisture level of about 10±1% (d.b.) was attained. Table 1 renders a detailed description of the drying programs at the constant air velocity of 0.6 m s^{-1}. The experimental results comparing the effects of single and combined applications of cold plasma and ultrasound waves on the air drying of cumin seeds were analyzed against a control group.

Measured Parameters

Drying Time (DT)

This study utilizes a first-order kinetic model to describe the moisture transfer during the drying process of cumin seeds, providing essential experimental data on drying kinetics, as follows (X. Wang *et al.*, 2023):

$$MR = \frac{Mt - M_e}{M_0 - M_e} \quad (1)$$

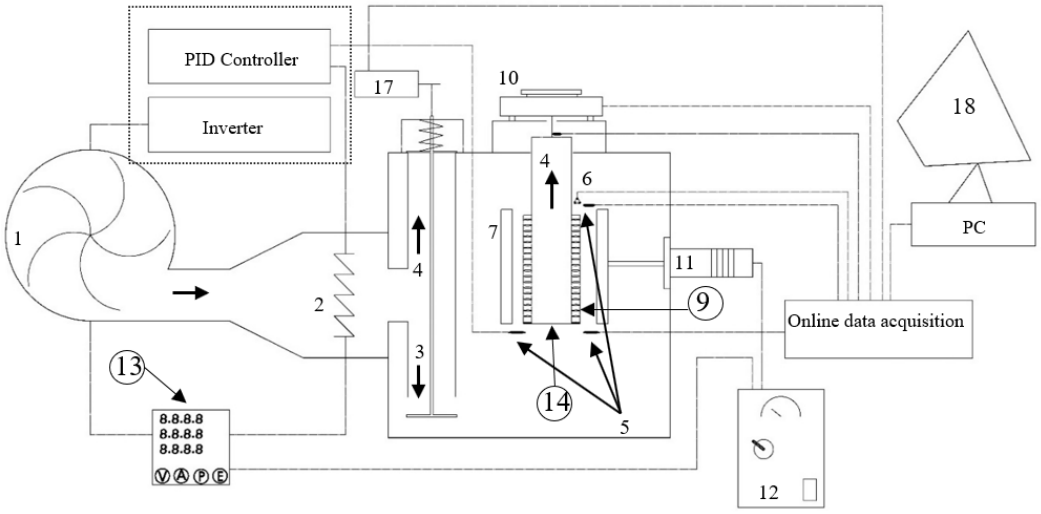

Fig. 1. A schematic view of the developed ultrasound assisted air dryer: 1- Centrifugal fan, 2- Thermal element, 3- Air in, 4- Air out, 5- Temperature and relative humidity sensor, 6- Laser sighting infrared sensor, 7- Cylindrical vibrating element (ultrasonic horn), 8- Cylindrical drying chamber, 9- Mesh screen, 10- Digital balance, 11- Ultrasonic transducer, 12- Ultrasonic generator, 13- Power meter, 14- Drying samples, 15- PID controller, 16- Electrical panel, 17- Gearbox DC motor, and 18- Monitor (Namjoo, Moradi, Dibagar, & Niakousari, 2022)

Table 1- A detailed description of the different seed drying programs designed for this research

Program description	Drying program	Drying air temperature (T)	Ultrasound power (USp)	Cold plasma pretreatment time (CPt)
Convective drying (Control group)	CV	30, 35, and 40 ˚C	0	0
Convective drying assisted by ultrasound waves	USCV	30, 35, and 40 ˚C	60, 120, and 180 W	0
Convective drying with cold plasma pretreatment	CPCV	30, 35, and 40 ˚C	0	15 and 30 s
Convective drying assisted by ultrasound waves with cold plasma pretreatment	CPUSCV	30, 35, and 40 ˚C	60, 120, and 180 W	15 and 30 s

Where, MR is the moisture ratio (-), M is the moisture content (% d.b.), and subscripts t, e, and 0 describe the instantaneous, equilibrium, and initial values, respectively. The experiments were performed to acquire data for the seed's moisture content as a function of time. Cumin seeds with an initial moisture content of 69.4±1% (d.b.) were dried to reach the final moisture level of 10±1% (d.b.). The required time was recorded in the drying program as the drying duration.

Effective Moisture Diffusivity (D_{eff})

Fick's second law was used to determine effective moisture diffusivity as suggested in the papers on drying foods. Here, the effective moisture diffusivity of the drying body was calculated by establishing a graphical method and assuming one-dimensional moisture movement, uniform initial moisture distribution, negligible shrinkage, and constant diffusion coefficient. The actual geometry of the drying body was a cylindrical mesh basket with the thickness and height of 8 and 130 mm, respectively, which was assumed similar to a rectangular slab with an airflow perpendicular to the samples. Therefore, the analytical solution for the drying body as a slab object is given in Eq. (2) (Chatzilia, Kaderides, & Goula, 2023; Lingayat, VP, & VRK, 2021):

$$MR = \frac{8}{\pi^2}\sum_{n=0}^{\infty}\frac{1}{(2n+1)^2}\exp\left(\frac{-(2n+1)^2\pi^2 D_{eff}.t}{4L^2}\right) \quad (2)$$

where L represents half of the thickness of the drying body (m), and n is a positive integer that stands for drying terms. By substituting n= 0 into Eq. (2), an excellent proximate solution is given in long drying times as follows (Gong *et al.*, 2020):

$$\ln(MR) = \ln\left(\frac{8}{\pi^2}\right) - \left(\frac{\pi^2 D_{eff}.t}{4L^2}\right) \quad (3)$$

The effective moisture diffusivity (D_{eff}) is typically established by a graphical method. This way, the experimental result is presented in terms of the natural logarithm of the moisture ratio (MR) as a function of drying time, as displayed in Eq. (4). The outcome is a linear regression ($A\times k_1+B$), in which the slope of the line (k_1) is used to compute the effective moisture diffusivity as follows (Dibagar, Kowalski, Chayjan, & Figiel, 2020):

$$k_1 = -\frac{\pi^2 D_{eff}}{4L^2} \quad (4)$$

Energy Consumption (EC)

In this research, energy consumption refers to the energy, which was supplied for the electrical elements of the main drying system, including fan, heating unit, sonication unit, etc. This amount of energy is required to remove water from the cumin seeds and attain the final moisture content of 10% (d.b.) in each experimental run. In this regard, a Power Meter instrument (Model Delta power, Ziegler Co., Germany) was utilized, and the consumed energy was directly recorded in kilowatt-hours (kWh).

Total Color Change (ΔE)

A new colorimetric system was employed to characterize the color quality of the fresh and dried cumin seeds. The color was determined using image processing technique. To ensure an acceptable image quality, a good camera and proper illumination were applied. The device, developed for measuring total color change, consisted of four main elements of a rectangular chamber (35 ×25 ×25 cm), sample holder, camera (Canon EOS 4000D) with three detectors per pixel: Red, Green, and Blue, and LED lamps. After locating the fresh and dried samples on the holder in the chamber's center, digital images were captured by the camera from the top. The images were then stored on a PC and processed with algorithms written in the toolbox of MATLAB R2013a to translate the color space of RGB to the reference zone L^* (whiteness/darkness), a^* (redness/greenness), and b^* (yellowness/blueness), followed by calculating the change in the color values of samples (ΔE) as follows (Izli & Polat, 2019; Özkan Karabacak, 2019):

$$\Delta E = \sqrt{(L^* - L_0^*)^2 + (a^* - a_0^*)^2 + (b^* - b_0^*)^2} \quad (5)$$

where, index 0 denotes the color specifications of the fresh cumin seeds. Higher values of ΔE stand for the significant difference between the color of fresh and dried seed samples.

Rupture Force (RF)

The spice industry relies on the size reduction of herbaceous plants, achieved through various forces to create particles with precise shapes and dimensions. Size reduction, one of the most energy-consuming processes in the food industry, is directly linked to microbiological and chemical stability and convenience (Saiedirad & Mirsalehi, 2010). Rupture force is defined as the amount of force needed to trigger the rupture of a product. It is related to the firmness and brittleness of the sample (Saiedirad *et al.*, 2008). The rupture force of the dried cumin seeds was assessed by an Instron Universal Testing Machine (Model STM-20, SANTAM Co., Iran) equipped with a compression load cell (Model DBBP-20, BONGSHIN Co., Korea), with an accuracy of ±0.01 N in force and ±0.001 mm in deformation. The mechanical test was repeated ten times for each drying point and reported in N.

Artificial Neural Network Modeling

The MLPNN training

The well-known multilayer perceptron neural network (MLPNN) is schematically described in Fig. 2. As can be seen, different layers with several neurons are considered in this model. The adjacent neurons are connected by weights (w_{ij}). The weights are corrected in an iterative back-propagation algorithm and in each iteration (q) are estimated as follows (Habibi & Nematollahi, 2019; Moosavi, Nematollahi, & Rahimi, 2021; Nematollahi, Jamali, & Hosseini, 2020; Nematollahi & Mousavi Khaneghah, 2019; Sun *et al.*, 2019; Zakeri, Naghavi, & Safavi, 2009):

$$w_{ij}(q+1) = w_{ij}(q) + \Delta w_{ij}(q) \quad (6)$$

In order to minimize the error in prediction of output variables, the generalized delta-learning rule is employed, and the following equation is proposed for computing the values of $\Delta w_{ji}(q)$:

$$\Delta w_{ji}(q) = \gamma f_j'(.) x_i \sum_{k=1}^{K} \{[(P_m)_k - (P_p)_k] f_k'(.) w_{kj}(q)\} + \alpha \Delta w_{ji}(q-1) \quad (7)$$

where P_p is the value predicted by NN, P_m is the experimentally measured data, and γ is the learning rate. The derivative of transfer function relative to its input variable x_i is denoted by $f'(.)$, and α is the momentum value and is a positive number between 0 and 1.

The RBFNN training

In the radial basis function neural network (RBFNN), two feed-forward layers are used for fast training of NNs. RBFNN considers the Gaussian basis function φ for weighted sum of input data vector $\mathbf{X}$. Then, the components of output vector Y_k are computed as (Nematollahi & Mousavi Khaneghah, 2019):

$$Y_k(\mathbf{X}) = \sum_{j=1}^{n} w_{kj} \varphi_j(\|\mathbf{X} - U_j\|) + b_k \quad (8)$$

Where, U is the vector of center of basis function φ.

The WNN training

The WNN is developed based on wavelet basis functions for training data and estimating the outputs. The wavelet algorithm is not iterative and compared to the conventional MLPNN, the learning time and the accuracy of the results improve greatly. The employed basis functions also allow for inclusion of multiresolution frameworks in the structure of WNN (Safavi & Romagnoli, 1997).

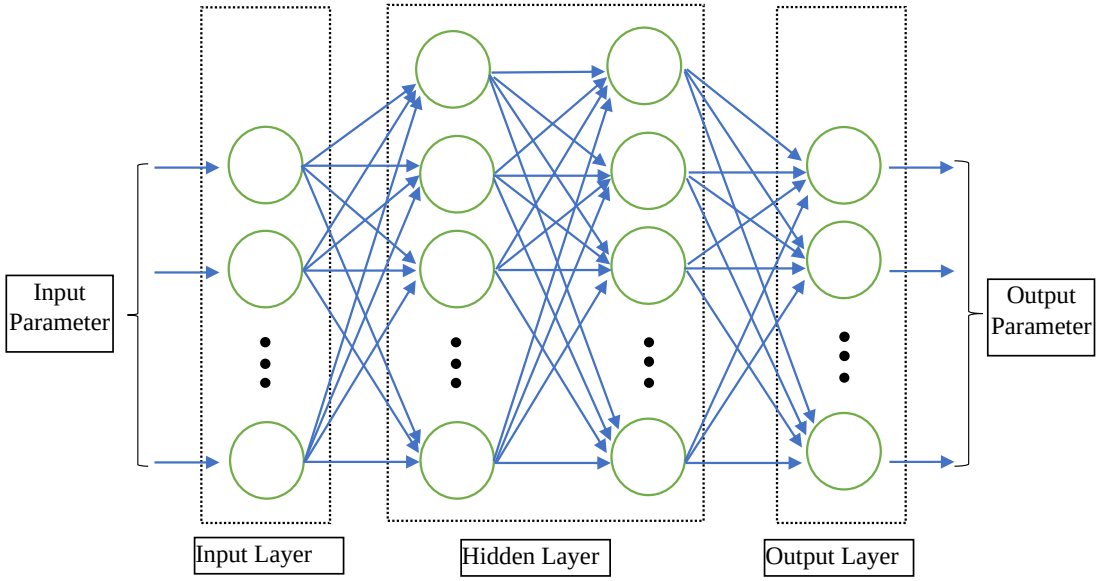

Fig. 2. Schematic illustration of the multilayer perceptron neural networks (MLPNNs).

In the WNN approach, the outputs of any function $\mathbf{F}(\mathbf{X}) \in L^2(R)$ are estimated as:

$$\mathbf{F}(\mathbf{X}) = \sum_{s=-\infty}^{s=+\infty} a_{0,s}\phi_{0,s}(\mathbf{X}) + \sum_{r=-\infty}^{0}\sum_{s=-\infty}^{s=+\infty} d_{r,s}\psi_{r,s}(\mathbf{X}) \quad (9)$$

Where $a_{0,s}$ and $d_{r,s}$ are constant coefficients, and the scaling functions $\phi_{r,s}$ and the wavelet functions $\psi_{r,s}$ are given by:

$$\psi_{r,s}(\mathbf{X}) = 2^{-r/2}\psi(2^{-r/2}\mathbf{X} - s) \quad r, s \in Z \quad (10)$$

$$\phi_{r,s}(\mathbf{X}) = 2^{-r/2}\phi(2^{-r/2}\mathbf{X} - s) \quad r, s \in Z \quad (11)$$

in which r and s are, respectively, the dilation and translation factors.

In order to evaluate the unknown coefficients "*a*" and "*d*", Safavi and Romagnoli (1997) rearranged Eq. (9) into the following form:

$$\mathbf{F}(\mathbf{X}) - \mathbf{F}_r(\mathbf{X}) = \sum_{s=-\infty}^{s=+\infty} c_{r,s}\theta_{r,s}(\mathbf{X}) \quad (12)$$

Then the set of linear equations were derived for the problem from:

$$\bar{\mathbf{F}}(\mathbf{X}) = \mathbf{AC} \quad (13)$$

Where,

$$\bar{\mathbf{F}} = \begin{bmatrix} \bar{\mathbf{F}}(\mathrm{X}_1) \\ \bar{\mathbf{F}}(\mathrm{X}_2) \\ \vdots \\ \bar{\mathbf{F}}(\mathrm{X}_n) \end{bmatrix}, \quad \mathbf{A} = \begin{bmatrix} \theta_1(\mathrm{X}_1) & \cdots & \theta_k(\mathrm{X}_1) \\ \vdots & & \vdots \\ \theta_1(\mathrm{X}_n) & \cdots & \theta_k(\mathrm{X}_k) \end{bmatrix}, \quad \mathbf{C} = \begin{bmatrix} c_1 \\ c_2 \\ \vdots \\ c_k \end{bmatrix} \quad (14)$$

The variable θ in Eq. (14) includes both scaling and wavelet functions. As a result, the vector *C* is found as:

$$\mathbf{C} = ((\mathbf{A}^{\mathrm{T}}\mathbf{A})^{-1}\mathbf{A}^{\mathrm{T}})\bar{\mathbf{F}} = \mathbf{A}^{+}\bar{\mathbf{F}} \quad (15)$$

Where A^{+} denotes the pseudo-inverse of matrix $\mathbf{A}$.

For more details about the WNN methodology and its training process, one could refer to. Figure 3 clearly shows the training process in WNN.

Multiple Quadratic Regression (MQR) Analysis

In addition to artificial neural networks, the Multiple Quadratic Regression (MQR) method is also used in this study to develop the predicting models. In this regard, the performance of the drying system, described by output variables y, is correlated by the following expression to the input parameters x_i (CPt, T and USp):

$$y = \beta_{11}x_1^2 + \beta_{22}x_2^2 + \beta_{33}x_3^2 + \beta_{12}x_1x_2 + \beta_{13}x_1x_3 + \beta_{23}x_2x_3 + \beta_1x_1 + \beta_2x_2 + \beta_3x_3 + \beta_0 \quad (16)$$

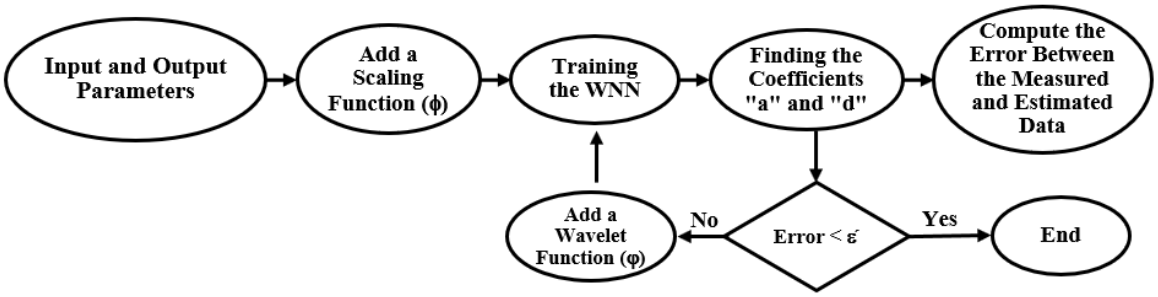

Fig. 3. The training process in WNN

where β_0 is a constant, and β_i , β_{ii} , and β_{ij} are the linear, pure quadratic, and interaction coefficients, respectively (Namjoo, Golbakhshi, Kamandar, & Beigi, 2024).

All aforementioned numerical modeling types were carried out using MATLAB software (Matlab, 2016). In order to develop and validate the models, 80% of the experimentally measured data was used for training and the remaining 20% was used for the test phase.

ANN and MQR Models Validation

To show the goodness of fit and performance of the used models, indices of the correlation coefficient (R), root mean square error (RMSE), the mean absolute percentage error (MAPE), and the mean absolute error (MAE) were calculated using Eqs. (17)-(20), respectively (Wang, Tian, & An, 2022).

$$R = \frac{\sum_{i=1}^{n}(Y_{pre\,i}-\overline{Y_{pre}})(Y_{exp\,i}-\overline{Y_{exp}})}{\sqrt{\sum_{i=1}^{n}(Y_{pre\,i}-\overline{Y_{pre}})^2 \sum_{i=1}^{n}(Y_{exp\,i}-\overline{Y_{exp}})^2}}, \quad (17)$$

i=1,2,3,.., N

$$RMSE = \left[\frac{1}{n}\sum_{i=1}^{n}(Y_{pre\,i} - Y_{exp\,i})^2\right]^{\frac{1}{2}}, \quad (18)$$

i=1,2,3,.., N

$$MAPE = \frac{1}{n}\sum_{i=1}^{n}\left|\frac{Y_{pre\,i}-Y_{exp\,i}}{Y_{exp\,i}}\right| \times 100, \quad (19)$$

i=1,2,3,.., N

$$MAE = \frac{1}{n}\sum_{i=1}^{n}\left|Y_{pre,i} - Y_{exp,i}\right|, \quad (20)$$

$$i = 1,2,3,..,N$$

where, $Y_{exp,i}$ and $Y_{pre,i}$ denote the i[th] experimental (measured) and predicted values, respectively. $\overline{Y_{exp}}$ and $\overline{Y_{pre}}$ are the corresponding mean values of $Y_{exp,i}$ and $Y_{pre,i}$, respectively. High values of R and lower RMSE, MAPE, and MAE outcomes confirm that the proposed model fits well to the experimental drying data, and it can be applied for prediction (Dotto, Souza, Simoes, Morejon, & Moreira, 2017; Nematollahi & Mousavi Khaneghah, 2019).

Results and Discussion

The experimental drying data underwent statistical analysis using IBM SPSS software (version 26). Statistical assessment of the results was performed using a factorial design to find the effect of drying air temperature (T) at three levels (30, 35, and 40 ºC), CPt at three levels (0, 15, and 30 s) and USp at four levels (0, 60, 120, and 180 W) on drying time, effective moisture diffusivity, energy consumption, total color change, and rupture force of dried cumin seeds during drying (Table 2). The experiment was conducted in a complete randomized design (CRD) with three replicates. The degree of freedom, sum squares, means squares, and F-values of the individual linear and interaction terms of CPt, T, and USp were generated through the analysis of variance (ANOVA) table. Additionally, the significance of each program evaluated was analyzed using ANOVA, with the results presented in Table 2.

Table 2- ANOVA results for the main and interaction effects of CPt, T, and USp on the studied parameters.

S.O.V.	D.F.	DT	D_{eff}	EC	ΔE	RF
CPt	2	13758.176**	1.910E-7**	1.152**	114.093**	316.732**
T	2	16289.065**	3.694E-7**	1.604**	11.901**	18.307**
USp	3	16952.012**	1.524E-7**	1.386**	9.916**	464.006**
USp×T	4	136.343*	1.197E-8**	0.017*	0.942*	4.286**
CPt×USp	6	1698.744**	1.101E-8**	0.077**	0.491^{ns}	25.624**
CPt×T	6	1489.262**	4.717E-9**	0.125**	0.468^{ns}	4.267**
CPt×T×USp	12	71.577^{ns}	1.628E-9^{ns}	0.018**	0.066^{ns}	0.250^{ns}
Error	72	51.167	1.329E-9	0.005	0.318	0.990
Total	107					

**: significant at 0.01, *: significant at 0.05, and ^{ns}: not significant

Results of the WNN, MLPNN, RBFNN, and MQR models

In this research, we aimed to develop some predicting models for correlating the inputs parameters (CP exposure time, drying air temperature, and ultrasound power) and outputs variables (drying time, effective moisture diffusivity, energy consumption, total color change, and rupture force). These models can readily reveal the optimal dehydration process for cumin seeds. In this regard, three well-known neural networks-based models, namely the MLPNN, RBFNN, and WNN were employed.

In order to minimize the error of MLPNN predictions, sufficient number of hidden layers and neurons should be considered for the architecture of network. In this regard, two hidden layers were used, and the sigmoid function was adopted as the transfer function. In an iterative learning procedure, the number of included neurons was systematically increased for improving the accuracy of predictions. The training process for the network was conducted using the Levenberg–Marquardt algorithm. Then it was found that by using 11 neurons within the hidden layers, acceptable accuracy may be achieved and adding more neurons did not provide any significant contribution.

To calibrate the outputs of the model with the prepared experimental data, the WNN model should be trained by selecting appropriate wavelet and examining different layers of resolution. In the special case of cumin seed drying, the second resolution and the Gaussian type wavelet were found to be the optimal parameters for the WNN.

The performances of WNN, MLPNN, and RBFNN, along with the regression-based MQR model, were evaluated, and their results are given in Table 3. As can be seen, MQR failed to provide accurate predictions, especially very poor results were obtained in this model for the total change in color of dried samples. MLP and RBF models provided sufficient estimations for drying time and energy consumption. However, the average accuracy of MLP was 2.28% better than that achieved in the RBF model. In this study, the most accurate predictions for the performance of drying system were evaluated by the WNN model. The average accuracy of results in WNN for all defined output variables was 3.02% and 5.37% better than MLP and RBF models, respectively. Furthermore, WNN enjoys a non-iterative learning algorithm for training neural networks. This greatly reduces the computational time and provides an important advantage for WNN. Therefore, in the subsequent sections of this paper, we used a WNN model for evaluating the effects of various input parameters on drying time, effective moisture diffusivity, energy consumption, total color change, and rupture force of dried seeds.

Table 3- The performance of the applied MQR and ANN models in prediction of cumin seeds drying parameters.

ANN models	Output variable	R^2		RMSE		MAPE		MAE	
		Train	Test	Train	Test	Train	Test	Train	Test
WNN	DT	0.9767	0.9399	5.9701	7.8990	2.0350	3.3251	4.5388	7.1591
	D_{eff}	0.9532	0.8943	$2.4736e^{-10}$	$3.4032e^{-10}$	2.0416	3.6538	$1.3357e^{-10}$	$1.9685e^{-10}$
	EC	0.9718	0.9251	0.0596	0.0797	1.7936	2.0066	0.0473	0.0478
	ΔE	0.9341	0.8339	0.5929	0.8167	3.0305	3.5292	0.3686	0.4643
	RF	0.9532	0.8943	0.3403	0.24736	2.0416	3.0538	0.2519	0.5418
	Avg.	0.9577	0.8971	1.39258	1.808552	2.18846	3.1137	1.04132	1.6426
MLP	DT	0.9681	0.9239	6.3331	8.9526	2.4853	3.522	5.1258	7.2562
	D_{eff}	0.9264	0.8679	0.2274×10^{-9}	0.1895×10^{-9}	2.4963	3.8158	0.1387×10^{-9}	0.1732×10^{-9}
	EC	0.9602	0.9065	0.0650	0.0834	3.1129	2.3476	0.0666	0.0505
	ΔE	0.9256	0.9076	0.5282	0.4661	4.1017	3.6409	0.3694	0.4817
	RF	0.9080	0.8214	1.1574	0.858	2.2521	3.1619	0.9851	0.6942
	Avg.	0.9296	0.9523	2.6804	1.93055	3.40526	2.64444	2.181225	1.559975
RBF	DT	0.9415	0.9594	9.5866	6.4513	4.2339	2.8297	8.5242	5.4283
	D_{eff}	0.8970	0.9378	0.2704×10^{-9}	0.1677×10^{-9}	3.8022	2.9022	0.2878×10^{-9}	0.1776×10^{-9}
	EC	0.9308	0.9430	0.1879	0.1461	3.5674	2.6835	0.124	0.0947
	ΔE	0.8712	0.9183	0.8764	0.6352	5.5838	3.9035	0.7387	0.5475
	RF	0.9050	0.9528	1.8599	0.9688	4.1379	2.7375	1.2427	0.8326
	Avg.	0.9089	0.9422	3.1277	2.05035	4.26504	3.01128	2.6574	1.725775
MQR	DT	0.8379	0.8477	13.7969	12.9660	5.4473	5.4126	11.4930	10.6436
	D_{eff}	0.8325	0.8425	3.27×10^{-10}	3.01×10^{-10}	4.9575	4.3275	2.63×10^{-10}	2.39×10^{-10}
	EC	0.8499	0.8574	0.1220	0.1168	4.4976	4.5901	0.0995	0.0961
	ΔE	0.7936	0.7916	0.7264	0.6798	6.0722	6.0306	0.6203	0.5824
	RF	0.8593	0.8763	1.7927	1.4871	4.6907	4.0843	1.4681	1.1990
	Avg.	0.83464	0.8431	3.2876	3.0500	5.1331	4.8890	2.736175	2.5042

Drying time

The neural network developed on the basis of WNN is used in this section for predicting the impact of various drying programs on the time duration of cumin seeds. As can be seen in Fig. 4, the R^2-values for the training and test data were found to be 0.9681 and 0.9432, respectively. This clearly indicates that the WNN model can properly predict the linear and complex correlations between drying time and the influential input variables. Our results are consistent with the outcomes reported in

earlier related studies. Specifically, the obtained R^2-values are in good agreement with the findings of Potisate *et al.* (2014) which varied between 0.81 and 0.98 across different drying treatments of moringa leaves.

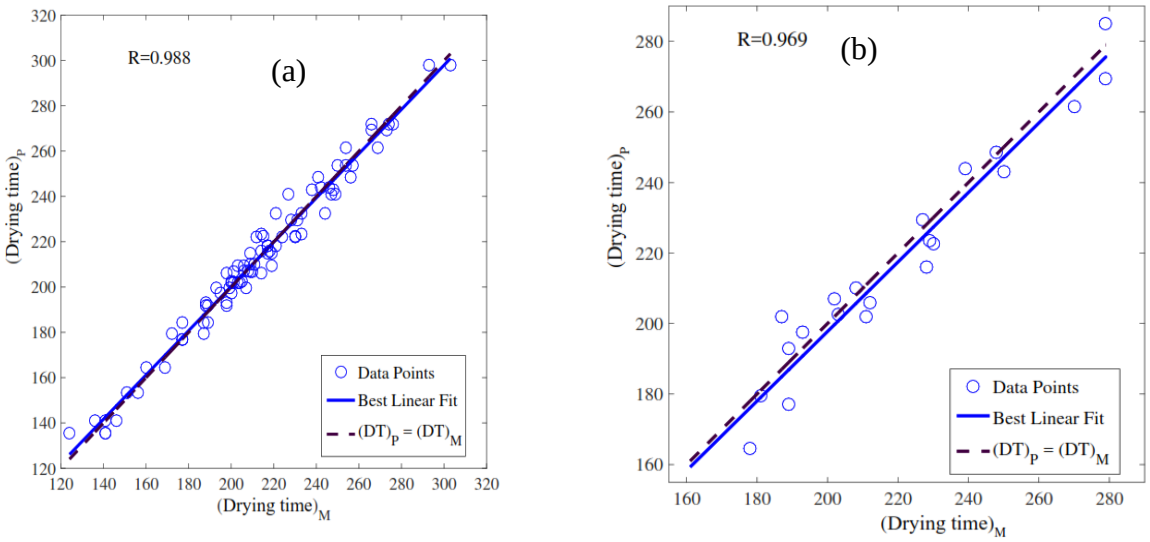

Fig. 4. The regression of the measured and predicted drying time: a) Train data, and b) Test data

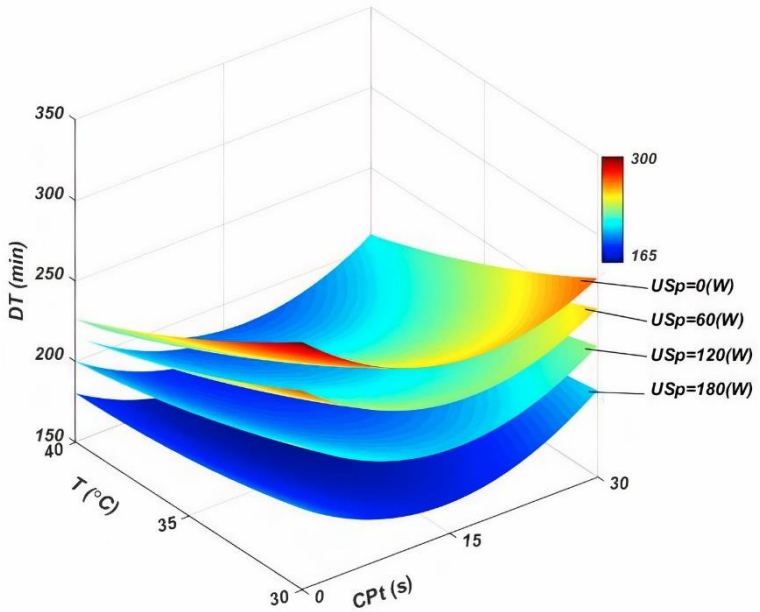

Fig. 5. Response surface plots for the effect of independent variables on drying time of cumin seeds during the drying process

The drying time of cumin seeds was assessed across various drying temperatures, USp, and CPt, with results presented in Fig. 5. In pure convective drying, drying times ranged from 219 to 293 minutes, with higher temperatures leading to faster drying. Introducing ultrasound waves accelerated drying, with total drying times ranging from 124 to 303 minutes, depending on temperature and ultrasound power. CPt before drying reduced drying times by 11.65% to 15.29% at various temperatures. Combining CP and ultrasound technologies further reduced drying times, with a minimum of 124 minutes

observed. However, longer CPt increased drying times due to surface hardening and increased evaporative resistance. Excessive CPt may disrupt cell walls and hinder water removal. Overall, CPt for 15 seconds significantly reduced drying times in an ultrasound-assisted system.

Effective moisture diffusivity

The results of the WNN model for effective moisture diffusivity were evaluated in Fig 6. The correlation coefficient (R^2) for train and test data was obtained as 0.9264 and 0.9421, respectively. Other introduced statistical measures were also used for further improvement of the model. To this end, the learning procedure continued until the values 0.2274×10^{-9}, 3.1278, and 0.1732×10^{-9} were attained, respectively, for the root mean square error (RMSE), mean absolute percentage error (MAPE), and mean absolute error (MAE). Then, RMSE, MAPE, and MAE were found to be 0.1895×10^{-9}, 2.4963, and 0.1387×10^{-9} for the test data, respectively. Similar conclusions were also made by Onwude *et al.* (2018) and Khanlari *et al.* (2020) for sweet potato and celery drying, respectively.

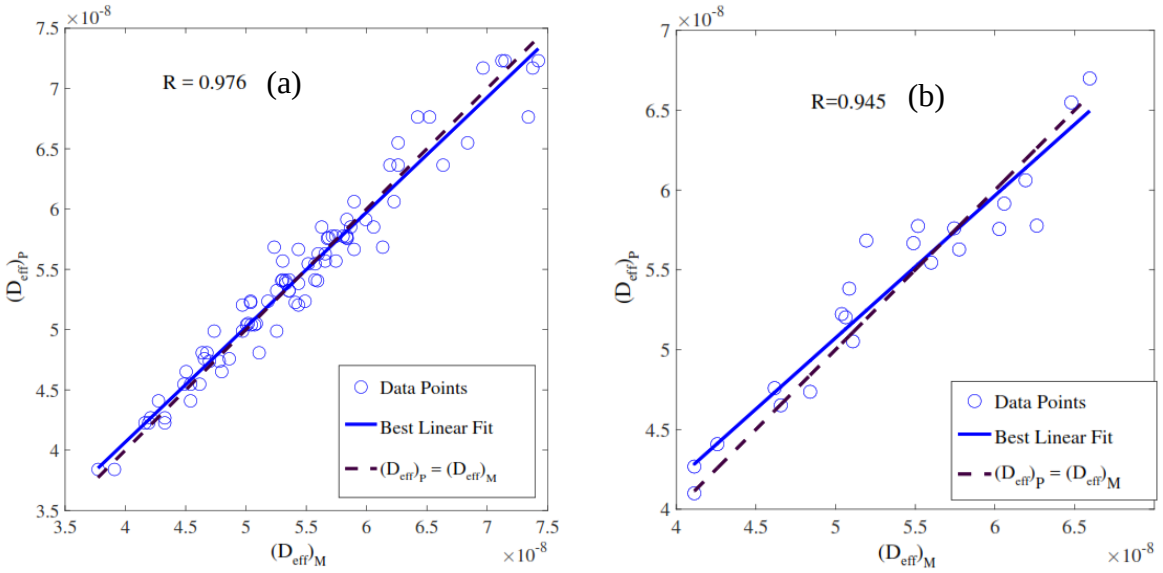

Fig. 6. The regression of the measured and predicted effective moisture diffusivity of cumin seeds: a) Train data, and b) Test data

Figure 7 illustrates the influence of various independent variables on enhancing the effective moisture diffusivity of samples. In a traditional drying setup, elevating the temperature resulted in increased seed diffusivity, reaching a maximum value of 9.29×10^{-10} m^2 s^{-1} at 40 °C, while the lowest diffusivity of 6.29×10^{-10} m^2 s^{-1} was observed at 30 °C.

In a combined drying system, varying ultrasound powers led to an increase in moisture diffusivity. The highest diffusivity (1.24×10^{-9} m^2 s^{-1}) was achieved at 40 °C with an ultrasound power of 180 W, while the lowest (7.51×10^{-10} m^2 s^{-1}) was observed at 30 °C with 60 W. Exposure to CP for 30 seconds enhanced seed moisture diffusivity. However, ultrasound power contributed more significantly to diffusivity enhancement at the same air temperatures, with longer exposure times (30 s) providing less modification. This suggests that excessive exposure to CP can increase diffusion resistance at the seed's surface.

Energy consumption

The results of experimental analysis for energy consumption were categorized into two test and train datasets and depicted in Figure 8. Two well-suited linear regression functions were proposed based on WNN. The error indices were evaluated in Table 3 for verifying

the predictions. As can be seen, RMSE, MAPE, and MAE for the training data are slightly more than those obtained for the test results. However, the correlation coefficient of results (R^2 = 0.9722 for train, and R^2 = 0.9254 for test data) demonstrated that the calculated values for energy consumption agree with the experimental results. The energetic investigations for drying of potato (Aghbashlo, Kianmehr, & Arabhosseini, 2008; Akpinar, Midilli, & Bicer, 2005), carrot slices (Nazghelichi, Kianmehr, & Aghbashlo, 2010), kodo millet grains, and fenugreek seeds (Yogendrasasidhar & Setty, 2018) also led to similar results.

Under different drying conditions, the results for energy consumption are given in Fig. 9. Various drying conditions were tested, and energy consumption was analyzed. In conventional convective drying, energy consumption ranged from 2.27 to 2.93 kWh, with lower temperatures resulting in higher energy usage due to longer drying times. Ultrasound-assisted drying showed a range of 1.95-2.93 kWh, with lower consumption at higher temperatures and ultrasound powers. Combining cold plasma pretreatment with ultrasound/convective drying significantly reduced energy usage to 1.42-2.85 kWh. CP pretreatment alone showed some energy savings, but the combination of CP and ultrasound provided the most efficient drying method, reducing energy consumption while maintaining product quality.

Color change

The results of experimental analysis and the WNN model for the change in color of dried seeds were illustrated in Fig. 10. The predictions of neural network for this variable had R^2 = 0.9256 for testing data, and R^2 = 0.9076 for training set. So, WNN can provide reliable predictions for the case which have not been experimentally investigated. Guiné *et al.* (2015), showed that for different drying treatments, artificial neural network modeling can precisely evaluate the color change of the banana variety. Bai *et al.* (2018) developed an ANNs model for investigating the drying kinetics and color changes of Ginkgo biloba seeds during microwave drying. The ANN models showed strong correlation to the experimental data, with correlation coefficients ranging from 0.956 to 0.9834. The models also had low mean square errors, between 0.0014 and 2.2044.

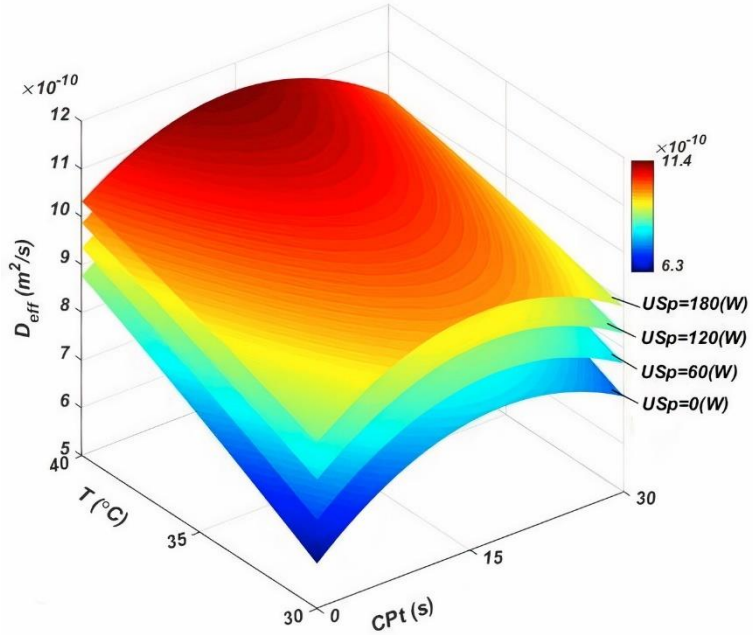

Fig. 7. Response surface plots for the effect of independent variables on moisture diffusivity of cumin seeds during the drying process

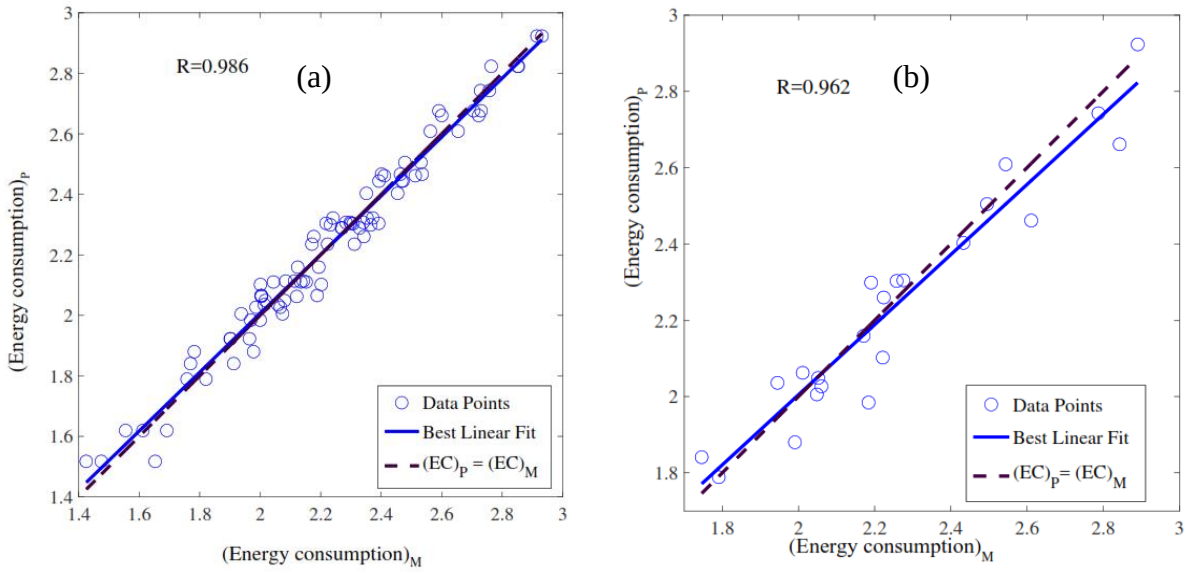

Fig. 8. The regression of the measured and predicted energy consumption: a) Train data, and b) Test data

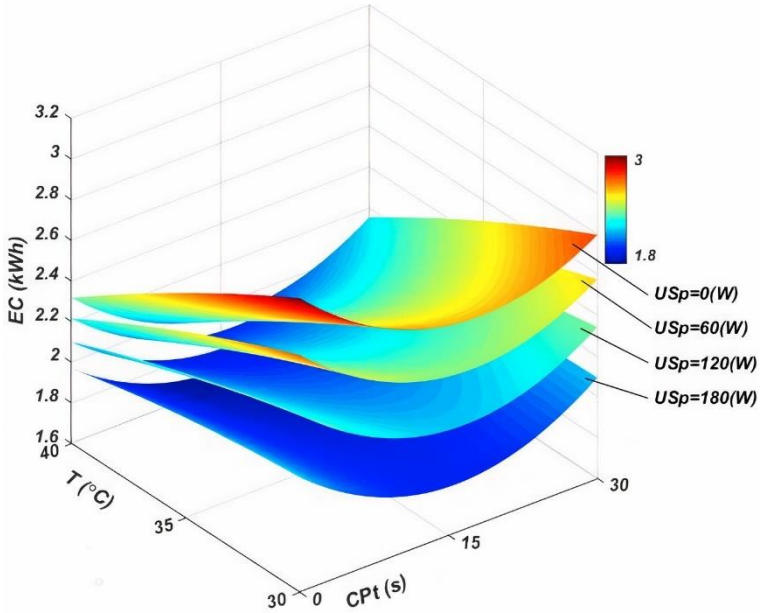

Fig. 9. Response surface plots for the effect of independent variables on the energy consumption of cumin seeds during the drying process

In this section, the changes in the color of cumin seeds were investigated, and the results were given in Fig. 11. In conventional drying, higher temperatures lead to greater color change, indicating potential degradation of quality. Introducing ultrasound reduces color change, with lower temperatures and higher ultrasound power showing the least change in color. CPt results in significant color change reduction, but prolonged exposure may have adverse effects. Combining CP pretreatment and ultrasound shows the most effective preservation of color, with minimal change observed at lower temperatures and higher ultrasound power. This indicates that integrating both CP and ultrasound technologies, while meticulously managing the parameters, presents the most effective method for maintaining seed quality.

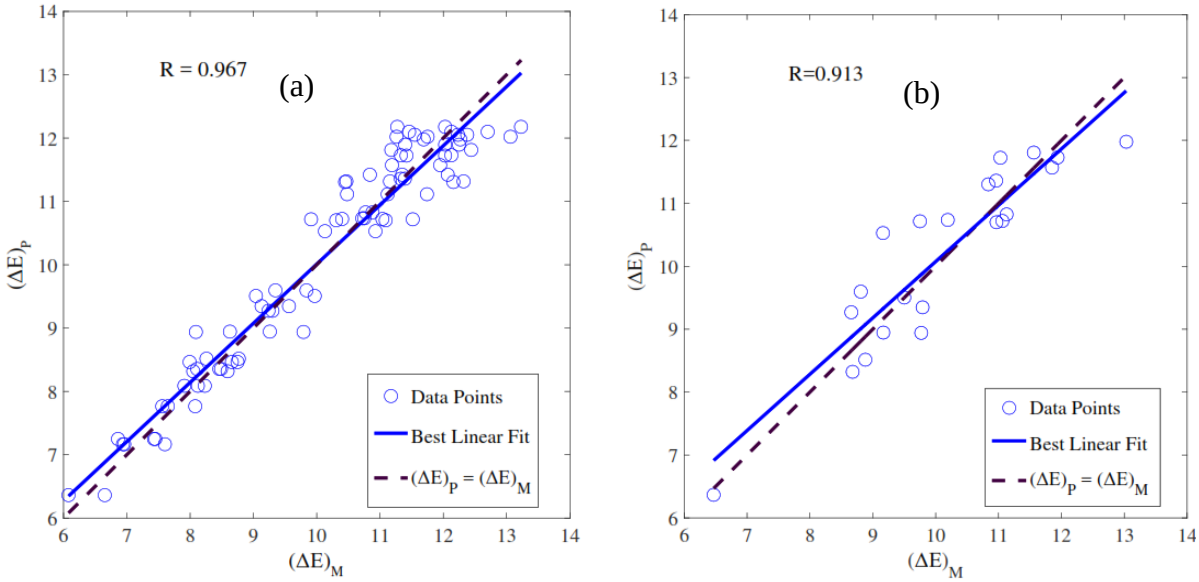

Fig. 10. The regression of the measured and predicted color change: a) Train data, and b) Test data

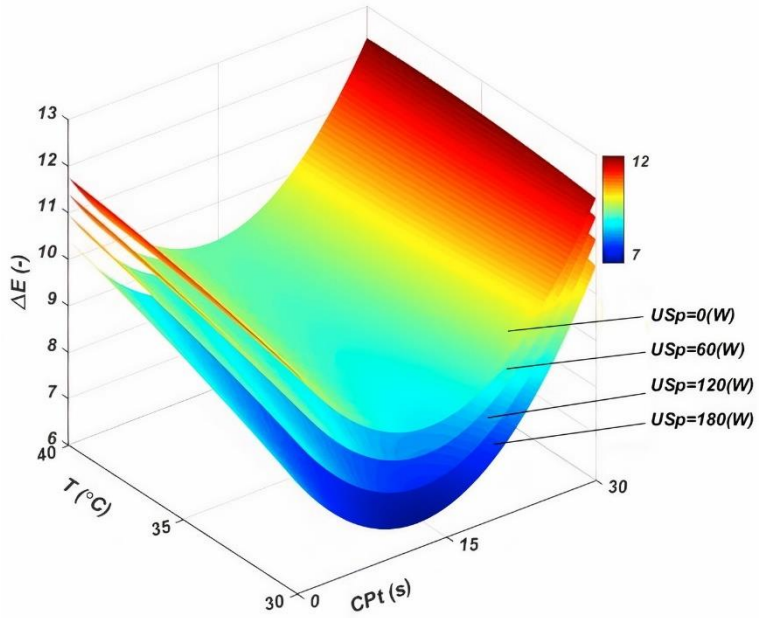

Fig. 11. Response surface plots for the effect of independent variables on the color change of cumin seeds during the drying process

Rupture force

The experimental data for the rupture force of dried seeds were displayed in Figure 12. Using the developed WNN model, the regression analysis was performed for mapping the input parameters with the desired variable. For both train and test datasets, the values of R^2 were found to be more than 0.90, and therefore best-fitting lines were proposed for the rupture force. The obtained values for RMSE, MAPE, and MAE (see Table 3) also reaffirmed that the WNN model suitably predicted the impact of drying conditions on the quality of end-products. The overall results are also found to be in very good agreement with the results of available investigations in the literature (Barreiro, Steinmetz, & Ruiz-Altisent, 1997; Saeidirad, Rohani, & Zarifneshat, 2013).

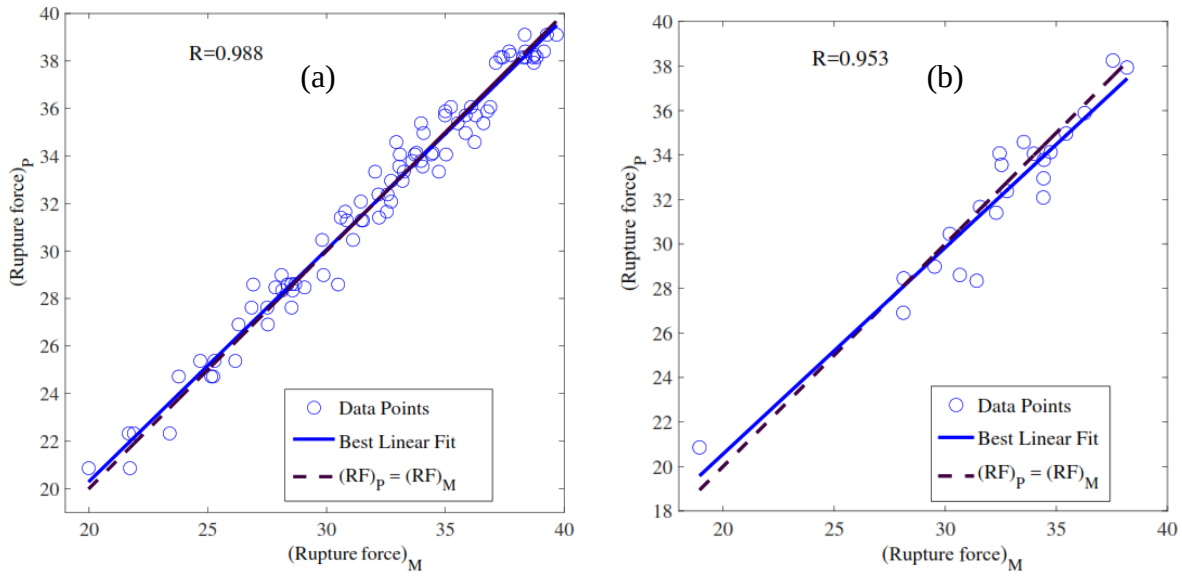

Fig. 12. The regression of the measured and predicted rupture force: a) Train data, and b) Test data

The effect of drying temperature, as well as exposing the seeds to US and CP, were evaluated and the results for the rupture force were given in Fig. 13. Convective drying temperatures showed minimal impact on seed crispiness. Introducing ultrasound led to cell collapse and increased ease of seed crushing. Higher ultrasound power resulted in significantly reduced rupture force. CPt had a lesser impact on reducing rupture force compared to ultrasound. Combining CPt with hybrid ultrasound/convective drying resulted in varying rupture forces depending on CP exposure time and ultrasound power. The scheme with CP pretreatment time of 15 seconds and ultrasound power of 180 W proved most effective in reducing rupture force.

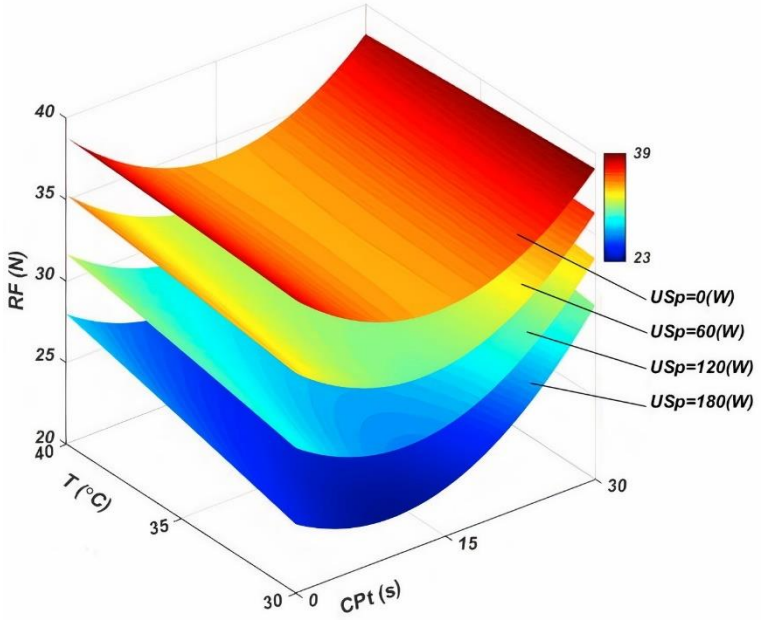

Fig. 13. Response surface plots for the effect of independent variables on the rupture force of cumin seeds during the drying process

Sensitivity analysis

Sensitivity analysis is a technique for evaluating the weight of each input parameter on output variables defined in the model. In this analysis, the inputs are systematically varying and the change in outputs are studied. This reveals which inputs inflict prominent impacts on the variation in outputs. Sensitivity analysis quantifies input uncertainty propagation and identifies influential parameters (Bhaskaran, Chennippan, & Subramaniam, 2020). In this section, the influence of input variables on DT, EC, ΔE, RF, and D_{eff} were studied, and the results were graphically shown in Fig. 14. It is evident that the drying temperature conveniently stimulated the moisture diffusivity D_{eff} but had no significant effects on the color change and rupture force.

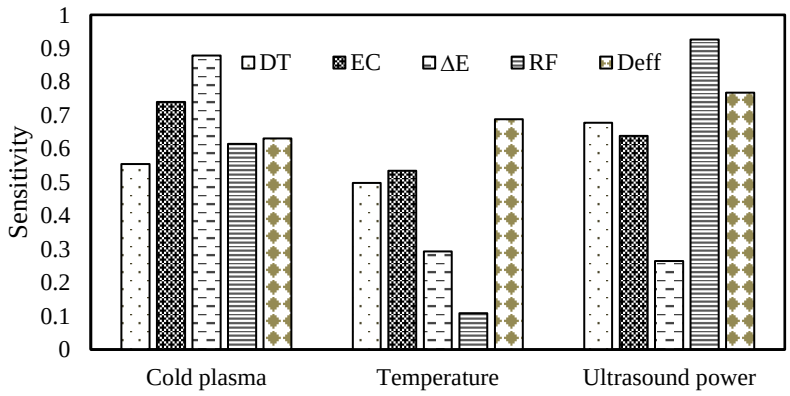

Fig. 14. Results of sensitivity analysis for hybrid drying of cumin seed

This raises the need for extra drying sources for improving the dehydration process. According to the results of sensitivity analysis, the average contribution of CP, temperature, and ultrasound to the output variables is 3.4176, 2.1227, and 3.2752, respectively. This clearly demonstrates the superiority of hybrid drying programs to the pure hot-air convective drying, and the CP was recognized as the most prominent factor. The maximum improvement in energy consumption EC and color change ΔE were created by exposing the seeds to CP. However, Fig. 9 shows that the ultrasound provided 21.73 and 50.73% more increase in D_{eff} and RF compared with those achieved CP. But contrary to CP, the ultrasonic power also had a negligible effect on the color change of cumin seed during the drying process.

Conclusion

In this study, some numerical predicting models were developed for investigating the contribution of cold plasma and high-power ultrasound waves for improving the convective air drying of cumin seeds. Three neural network models, namely MLPNN, RBFNN, and WNN, were used for predicting the performance of drying systems. The drying air temperature, CP exposing time, and the sonication power were selected as the input variables. The dehydration process was described by drying time, effective moisture diffusivity, energy consumption, color change, and the rupture force of dried seeds. The available experimental data was used for training and testing the models. The results of the regression-based MQR model were also evaluated and compared with the results of neural network models. Among all developed models, MLPNN and WNN showed the best fitting with the experimental data. The average values of R^2 = 0.9523 and RMSE = 1.93055 were found for the results of MLPNN, while the error indices obtained for the predictions of

WNN were estimated as R^2 = 0.8972 and RMSE = 1.808552. However, the WNN model used a non-iterative learning algorithm with a significantly shorter computational time. Therefore, this model was recognized as the most appropriate predicting tool for investigating the hybrid convective drying of cumin seeds.

Data availability statement

The data that support the findings of this study are available from the corresponding author, upon reasonable request.

Declaration of competing interests

The authors declare that they have no conflict of interest.

Authors Contribution

M. Namjoo: Data acquisition, Data pre and post processing, Writing- Original draft, Statistical analysis.

M. Moradi: Supervision, Technical advice, Review and editing services

M. A. Nematollahi: Numerical/computer simulation, Validation, Writing- Original draft

H. Golbakhshi: Review and editing services

References

1. Aghbashlo, M., Kianmehr, M. H., & Arabhosseini, A. (2008). Energy and exergy analyses of thin-layer drying of potato slices in a semi-industrial continuous band dryer. *Drying Technology*, *26*(12), 1501-1508. https://doi.org/10.1080/07373930802412231
2. Akpinar, E. K., Midilli, A., & Bicer, Y. (2005). Energy and exergy of potato drying process via cyclone type dryer. *Energy Conversion and Management*, *46*(15-16), 2530-2552. https://doi.org/10.1016/j.enconman.2004.12.008
3. Amini, G., Salehi, F., & Rasouli, M. (2021). Drying kinetics of basil seed mucilage in an infrared dryer: Application of GA-ANN and ANFIS for the prediction of drying time and moisture ratio. *Journal of Food Processing and Preservation*, *45*(3), e15258. https://doi.org/10.1111/jfpp.15258
4. Bai, J.-W., Xiao, H.-W., Ma, H.-L., & Zhou, C.-S. (2018). Artificial Neural Network Modeling of Drying Kinetics and Color Changes of Ginkgo Biloba Seeds during Microwave Drying Process. *Journal of Food Quality*, *2018*, 3278595. https://doi.org/10.1155/2018/3278595
5. Barreiro, P., Steinmetz, V., & Ruiz-Altisent, M. (1997). Neural bruise prediction models for fruit handling and machinery evaluation. *Computers and Electronics in Agriculture*, *18*(2-3), 91-103. https://doi.org/10.1016/s0168-1699(97)00022-7
6. Bhaskaran, P. E., Chennippan, M., & Subramaniam, T. (2020). Future prediction & estimation of faults occurrences in oil pipelines by using data clustering with time series forecasting. *Journal of Loss Prevention in the Process Industries*, *66*, 104203. https://doi.org/10.1016/j.jlp.2020.104203
7. Chatzilia, T., Kaderides, K., & Goula, A. M. (2023). Drying of peaches by a combination of convective and microwave methods. *Journal of Food Process Engineering*, *46*(4), e14296. https://doi.org/10.1111/jfpe.14296
8. Dhurve, P., Tarafdar, A., & Arora, V. K. (2021). Vibro-Fluidized Bed Drying of Pumpkin Seeds: Assessment of Mathematical and Artificial Neural Network Models for Drying Kinetics. *Journal of Food Quality*, *2021*, 7739732. https://doi.org/10.1155/2021/7739732
9. Dibagar, N., Kowalski, S. J., Chayjan, R. A., & Figiel, A. (2020). Accelerated convective drying of sunflower seeds by high-power ultrasound: Experimental assessment and optimization approach. *Food and Bioproducts Processing*, *123*, 42-59. https://doi.org/10.1016/j.fbp.2020.05.014
10. Dotto, G. L., Souza, T. B., Simoes, M. R., Morejon, C. F., & Moreira, M. F. P. (2017). Diffusive-convective model considering the shrinkage applied for drying of pears (*pyrus*). *Journal of Food Process Engineering*, *40*(4), e12503. https://doi.org/10.1111/jfpe.12503

11. Gong, C., Liao, M., Zhang, H., Xu, Y., Miao, Y., & Jiao, S. (2020). Investigation of hot air–assisted radio frequency as a final-stage drying of pre-dried carrot cubes. *Food and Bioprocess Technology, 13*(3), 419-429. https://doi.org/10.1007/s11947-019-02400-0
12. Guiné, R. P., Barroca, M. J., Gonçalves, F. J., Alves, M., Oliveira, S., & Mendes, M. (2015). Artificial neural network modelling of the antioxidant activity and phenolic compounds of bananas submitted to different drying treatments. *Food Chemistry, 168*, 454-459. https://doi.org/10.1016/j.foodchem.2014.07.094
13. Guo, Y.-R., An, Y.-M., Jia, Y.-X., & Xu, J.-G. (2018). Effect of drying methods on chemical composition and biological activity of essential oil from cumin (*Cuminum cyminum*). *Journal of Essential Oil Bearing Plants, 21*(5), 1295-1302. https://doi.org/10.1080/0972060x.2018.1538818
14. Habibi, S., & Nematollahi, M. (2019). Position and mass identification in nanotube mass sensor using neural networks. *Proceedings of the Institution of Mechanical Engineers, Part C: Journal of Mechanical Engineering Science, 233*(15), 5377-5387. https://doi.org/10.1177/0954406219841075
15. Izli, N., & Polat, A. (2019). Freeze and convective drying of quince (*Cydonia oblonga*): Effects on drying kinetics and quality attributes. *Heat and Mass Transfer, 55*, 1317-1326. https://doi.org/10.1007/s00231-018-2516-y
16. Kalathingal, M. S. H., Basak, S., & Mitra, J. (2020). Artificial neural network modeling and genetic algorithm optimization of process parameters in fluidized bed drying of green tea leaves. *Journal of Food Process Engineering, 43*(1), e13128. https://doi.org/10.1111/jfpe.13128
17. Kaveh, M., Abbaspour Gilandeh, Y., Amiri Chayjan, R., & Mohammadigol, R. (2019). Comparison of Mathematical Modeling, Artificial Neural Networks and Fuzzy Logic for Predicting the Moisture Ratio of Garlic and Shallot in a Fluidized Bed Dryer. *Journal of Agricultural Machinery, 9*(1), 99-112. https://doi.org/10.22067/jam.v9i1.66231
18. Kaveh, M., Chayjan, R. A., & Khezri, B. (2018). Modeling drying properties of pistachio nuts, squash and cantaloupe seeds under fixed and fluidized bed using data-driven models and artificial neural networks. *International Journal of Food Engineering, 14*(1), 10-23. https://doi.org/10.1515/ijfe-2017-0248
19. Khalo ahmadi, A., Roustapour, O. R., & Borghaee, A. M. (2022). Design and Construction of a Cabinet Dryer for Food Waste and Evaluation of its Kinetics and Energy Consumption. *Journal of Agricultural Machinery, 12*(4), 467-480. https://doi.org/10.22067/jam.2021.69918.1037
20. Khanlari, A., Güler, H. Ö., Tuncer, A. D., Şirin, C., Bilge, Y. C., Yılmaz, Y., & Güngör, A. (2020). Experimental and numerical study of the effect of integrating plus-shaped perforated baffles to solar air collector in drying application. *Renewable energy, 145*, 1677-1692. https://doi.org/10.1016/j.renene.2019.07.076
21. Lingayat, A., VP, C., & VRK, R. (2021). Drying kinetics of tomato (*Solanum lycopersicum*) and Brinjal (*Solanum melongena*) using an indirect type solar dryer and performance parameters of dryer. *Heat and Mass Transfer, 57*, 853-872. https://doi.org/10.1007/s00231-020-02999-3
22. Liu, Z.-L., Bai, J.-W., Wang, S.-X., Meng, J.-S., Wang, H., Yu, X.-L., ..., & Xiao, H.-W. (2019). Prediction of energy and exergy of mushroom slices drying in hot air impingement dryer by artificial neural network. *Drying Technology*. https://doi.org/10.1080/07373937.2019.1607873
23. Matlab, S. (2016). Matlab. *The MathWorks, Natick, MA*.
24. Meerasri, J., & Sothornvit, R. (2022). Artificial neural networks (ANNs) and multiple linear regression (MLR) for prediction of moisture content for coated pineapple cubes. *Case Studies in Thermal Engineering, 33*, 101942. https://doi.org/10.1016/j.csite.2022.101942

25. Merah, O., Sayed-Ahmad, B., Talou, T., Saad, Z., Cerny, M., Grivot, S., ..., & Hijazi, A. (2020). Biochemical composition of cumin seeds, and biorefining study. *Biomolecules*, *10*(7), 1054. https://doi.org/10.3390/biom10071054
26. Miraei Ashtiani, S.-H., Rafiee, M., Mohebi Morad, M., Khojastehpour, M., Khani, M. R., Rohani, A., ..., & Martynenko, A. (2020). Impact of gliding arc plasma pretreatment on drying efficiency and physicochemical properties of grape. *Innovative Food Science & Emerging Technologies*, *63*, 102381. https://doi.org/10.1016/j.ifset.2020.102381
27. Moghimi, M., Farzaneh, V., & Bakhshabadi, H. (2018). The effect of ultrasound pretreatment on some selected physicochemical properties of black cumin (*Nigella Sativa*). *Nutrire*, *43*(1), 1-8. https://doi.org/10.1186/s41110-018-0077-y
28. Moosavi, A. A., Nematollahi, M. A., & Rahimi, M. (2021). Predicting water sorptivity coefficient in calcareous soils using a wavelet–neural network hybrid modeling approach. *Environmental Earth Sciences*, *80*, 1-19. https://doi.org/10.1007/s12665-021-09518-5
29. Moradi, M., Ghasemi, J., & Azimi-Nejadian, H. (2021). Energy and Exergy Analysis of Drying Process of Lemon Verbena Leaves in a Solar Dryer. *Journal of Agricultural Machinery*, *11*(2), 423-433. https://doi.org/10.22067/jam.v11i2.85801
30. Namjoo, M., Dibagar, N., Golbakhshi, H., Figiel, A., & Masztalerz, K. (2024). RSM-Based Optimization Analysis for Cold Plasma and Ultrasound-Assisted Drying of Caraway Seed. *Foods*, *13*(19), 3084. https://doi.org/10.3390/foods13193084
31. Namjoo, M., Golbakhshi, H., Kamandar, M. R., & Beigi, M. (2024). Multi-Objective Investigation and Optimization of Paddy Processing in a Hot Air Dryer. *Periodica Polytechnica Chemical Engineering*. https://doi.org/10.3311/PPch.24100
32. Namjoo, M., Moradi, M., Dibagar, N., & Niakousari, M. (2022). Cold plasma pretreatment prior to ultrasound-assisted air drying of cumin seeds. *Food and Bioprocess Technology*, *15*(9), 2065-2083. https://doi.org/10.1007/s11947-022-02863-8
33. Namjoo, M., Moradi, M., Niakousari, M., & Karparvarfard, S. H. (2022). Ultrasound-assisted air drying of cumin seeds: modeling and optimization by response surface method. *Heat and Mass Transfer*. https://doi.org/10.1007/s00231-022-03306-y
34. Nazghelichi, T., Kianmehr, M. H., & Aghbashlo, M. (2010). Thermodynamic analysis of fluidized bed drying of carrot cubes. *Energy*, *35*(12), 4679-4684. https://doi.org/10.1016/j.energy.2010.09.036
35. Nematollahi, M. A., Jamali, B., & Hosseini, M. (2020). Fluid velocity and mass ratio identification of piezoelectric nanotube conveying fluid using inverse analysis. *Acta Mechanica*, *231*(2), 683-700.https://doi.org/10.1007/s00707-019-02554-0
36. Nematollahi, M. A., & Mousavi Khaneghah, A. (2019). Neural network prediction of friction coefficients of rosemary leaves. *Journal of Food Process Engineering*, *42*(6), e13211. https://doi.org/10.1111/jfpe.13211
37. Onwude, D. I., Hashim, N., Abdan, K., Janius, R., & Chen, G. (2018). Investigating the influence of novel drying methods on sweet potato (*Ipomoea batatas*): Kinetics, energy consumption, color, and microstructure. *Journal of Food Process Engineering*, *41*(4), e12686. https://doi.org/10.1111/jfpe.12686
38. Osloob, F., Moradi, M., & Niakousari, M. (2023). Cold Plasma: A Novel Pretreatment Method for Drying Canola Seeds: Kinetics Study and Superposition Modeling. *Journal of Agricultural Machinery*, *13*(1), 41-53. https://doi.org/10.22067/jam.2022.75630.1096
39. Özkan Karabacak, A. (2019). Effects of different drying methods on drying characteristics, colour and in-vitro bioaccessibility of phenolics and antioxidant capacity of blackthorn pestil (leather). *Heat and Mass Transfer*, *55*, 2739-2750. https://doi.org/10.1007/s00231-019-02611-3
40. Potisate, Y., Phoungchandang, S., & Kerr, W. L. (2014). The effects of predrying treatments and different drying methods on phytochemical compound retention and drying characteristics

of Moringa leaves (*Moringa oleifera*). *Drying Technology, 32*(16), 1970-1985. https://doi.org/10.1080/07373937.2014.926912
41. Rezaei, S., Behroozi-Khazaei, N., & Darvishi, H. (2021). Modeling of Potato Slice Drying Process in a Microwave Dryer using Artificial Neural Network and Machine Vision. *Journal of Agricultural Machinery, 11*(2), 263-275. https://doi.org/10.22067/jam.v11i2.78709
42. Saeidirad, M. H., Rohani, A., & Zarifneshat, S. (2013). Predictions of viscoelastic behavior of pomegranate using artificial neural network and Maxwell model. *Computers and Electronics in Agriculture, 98*, 1-7. https://doi.org/10.1016/j.compag.2013.07.009
43. Safavi, A. A., & Romagnoli, J. A. (1997). Application of wavelet-based neural networks to the modelling and optimisation of an experimental distillation column. *Engineering Applications of Artificial Intelligence, 10*(3), 301-313. https://doi.org/10.1016/S0952-1976(97)00009-2
44. Saiedirad, M., & Mirsalehi, M. (2010). Prediction of mechanical properties of cumin seed using artificial neural networks. *Journal of Texture studies, 41*(1), 34-48. https://doi.org/10.1111/j.1745-4603.2009.00211.x
45. Saiedirad, M., Tabatabaeefar, A., Borghei, A., Mirsalehi, M., Badii, F., & Varnamkhasti, M. G. (2008). Effects of moisture content, seed size, loading rate and seed orientation on force and energy required for fracturing cumin seed (*Cuminum cyminum*) under quasi-static loading. *Journal of Food Engineering, 86*(4), 565-572. https://doi.org/10.1016/j.jfoodeng.2007.11.021
46. Shashikanthalu, S. P., Ramireddy, L., & Radhakrishnan, M. (2020). Stimulation of the germination and seedling growth of Cuminum cyminum L. seeds by cold plasma. *Journal of Applied Research on Medicinal and Aromatic Plants, 18*, 100259. https://doi.org/10.1016/j.jarmap.2020.100259
47. Sun, Q., Zhang, M., & Mujumdar, A. S. (2019). Recent developments of artificial intelligence in drying of fresh food: A review. *Critical Reviews in Food Science and Nutrition, 59*(14), 2258-2275. https://doi.org/10.1080/10408398.2018.1446900
48. Tabibian, S. A., Labbafi, M., Askari, G. H., Rezaeinezhad, A. R., & Ghomi, H. (2020). Effect of gliding arc discharge plasma pretreatment on drying kinetic, energy consumption and physico-chemical properties of saffron. *Journal of food engineering, 270*, 109-117. https://doi.org/10.1016/j.jfoodeng.2019.109766
49. Wang, C., Tian, S., & An, X. (2022). The effects of drying parameters on drying characteristics, colorimetric differences, antioxidant components of sliced chinese jujube. *Heat and Mass Transfer, 58*(9), 1561-1571. https://doi.org/10.1007/s00231-023-03412-5
50. Wang, X., Zhong, J., Han, M., Li, F., Fan, X., & Liu, Y. (2023). Drying characteristics and moisture migration of ultrasound enhanced heat pump drying on carrot. *Heat and Mass Transfer*, 1-12. https://doi.org/10.1007/s00231-023-03564-1
51. Yogendrasasidhar, D., & Setty, Y. P. (2018). Drying kinetics, exergy and energy analyses of Kodo millet grains and Fenugreek seeds using wall heated fluidized bed dryer. *Energy, 151*, 799-811. https://doi.org/10.1016/j.energy.2018.03.089
52. Zakeri, V., Naghavi, V., & Safavi, A. A. (2009). Developing real-time wave-net models for non-linear time-varying experimental processes. *Computers & Chemical Engineering, 33*(8), 1379-1385. https://doi.org/10.1016/j.compchemeng.2009.02.003
53. Zhou, Y.-H., Vidyarthi, S. K., Zhong, C.-S., Zheng, Z.-A., An, Y., Wang, J., ..., & Xiao, H.-W. (2020). Cold plasma enhances drying and color, rehydration ratio and polyphenols of wolfberry via microstructure and ultrastructure alteration. *LWT, 134*, 110173. https://doi.org/10.1016/j.lwt.2020.110173

نشریه ماشین‌های کشاورزی
https://jame.um.ac.ir

مقاله پژوهشی
جلد ۱۵، شماره ۱، بهار ۱٤۰٤، ص ۲۲-۱

مدل‌سازی اثر توام پلاسمای سرد و توان فراصوت بر خشک شدن دانه‌های زیره سبز در یک خشک‌کن هوای گرم با استفاده از شبکه عصبی مصنوعی

مسلم نامجو [۱]، مهدی مرادی [۲*]، محمدامین نعمت اللهی [۲]، حسین گلبخشی [۳]

تاریخ دریافت: ۱۴۰۲/۰۹/۱۵
تاریخ پذیرش: ۱۴۰۳/۰۲/۲۲

چکیده

این مطالعه به‌منظور بررسی اثر زمان پلاسمای سرد (CPt) و توان امواج فراصوت (USp) بر خشک شدن دانه زیره سبز در یک خشک‌کن هوای گرم انجام شد. در این راستا، از یک دستگاه تولید پلاسمای سرد و یک خشک‌کن هیبریدی هوای گرم- فراصوت در مقیاس آزمایشگاهی استفاده شد و روش‌های خشک کردن به گونه‌ای برنامه‌ریزی شد که اثرات CPt و USp در خشک کردن دانه‌ها به‌صورت منفرد یا ترکیبی دخالت داشته باشند. زمان‌های مختلف پیش‌تیمار پلاسمای سرد (۱۵ و ۳۰ ثانیه)، توان‌های امواج فراصوت (۶۰، ۱۲۰ و ۱۸۰ وات) و دمای هوای خشک شدن (۳۰، ۳۵ و ۴۰ درجه سانتی‌گراد) برای مطالعه تغییرات زمان خشک کردن، ضریب نفوذپذیری مؤثر رطوبت، مصرف انرژی، تغییر رنگ کل، نیروی گسیختگی بذر زیره سبز انجام گرفت. از سه شبکه عصبی مصنوعی معروف شامل شبکه عصبی مبتنی بر موجک (WNN)، پرسپترون چندلایه (MLPNNs)، تابع پایه شعاعی (RBFNNs) و تحلیل رگرسیون چندگانه درجه دوم (MQR) برای مدل‌سازی ورودی‌های مذکور و پارامترهای خشک‌کردن استفاده شد. بر اساس نتایج مدل‌سازی، بهترین برازش خطی بین داده‌های تجربی و مقادیر پیش‌بینی‌شده توسط مدل‌سازی شبکه عصبی WNN با حداکثر R^2، ۰/۹۲ و ۰/۸۳ به‌ترتیب برای داده‌های آموزش و تست به‌دست آمد.

واژه‌های کلیدی: پلاسمای سرد، خشک کردن، دانه‌های زیره سبز، شبکه عصبی مصنوعی، فراصوت

۱- گروه مکانیک بیوسیستم، دانشکده کشاورزی، دانشگاه جیرفت، جیرفت، ایران
۲- گروه مهندسی بیوسیستم، دانشکده کشاورزی، دانشگاه شیراز، شیراز، ایران
۳- گروه مکانیک، دانشگاه جیرفت، جیرفت، ایران
(*- نویسنده مسئول: Email: moradih@shirazu.ac.ir)

https://doi.org/10.22067/jam.2024.85744.1209